Thermophysical properties of gaseous refrigerants from speed of sound measurements. I. Apparatus, model, and results for 1,1,1,2-tetrafluoroethane R134a

A. R. H. Goodwin[a] and M. R. Moldover[b]
Thermophysics Division, National Institute of Standards and Technology, Gaithersburg, Maryland 20899

(Received 1 March 1990; accepted 7 May 1990)

The speed of sound in gaseous 1,1,1,2-tetrafluoroethane (R134a) has been obtained between 233.16 and 340 K from measurements of the frequency of the radial acoustic resonances of a gas-filled spherical cavity. Perfect-gas heat capacities and second and third acoustic virial coefficients have been calculated from the results. The acoustic virial coefficients are used to estimate the density virial coefficients $B(T)$ and $C(T)$ and an effective square-well potential. The estimates of $B(T)$ are consistent with $B(T)$ deduced from high-quality equation-of-state measurements; those for $C(T)$ are slightly inconsistent. The apparatus and its calibration with argon are described.

I. INTRODUCTION

We report speeds of sound $u(p,T)$ in the refrigerant R134a (1,1,1,2-tetrafluoroethane) in the temperature range 233.16 to 340 K at pressures between 5.6 and 575 kPa. This range includes the normal boiling temperature of R134a, 246.65 K, but is below the critical temperature of 374.205 K.[1] From the speed-of-sound data, we deduce perfect-gas heat capacities, virial coefficients, and an effective square-well potential.

Following the Montreal Protocol[2] restricting environmentally unacceptable refrigerant production, R134a has emerged as a leading candidate to replace R12. To evaluate the utility of this proposed replacement, a complete set of thermophysical properties is required. The heat capacities reported here are the only ones obtained from measurements for R134a, and the virial coefficients are complementary to those determined from the precise $p(V_m,T)$ measurements of Weber[3] made on another portion of the same batch of R134a. The present measurements are one part of a major program to determine the thermophysical behavior of several alternative refrigerants. Some of the present results were included in an interim formulation[1] of the thermodynamic properties of R134a. We shall report speed-of-sound data for three other alternative refrigerants in the near future.

The present speed-of-sound results are shown in Fig. 1. They have been analyzed with the acoustic virial expansion:

$$u^2 = (RT\gamma_0/M)\left[1 + (\beta_a/RT)p + (\gamma_a/RT)p^2 + \cdots\right], \tag{1}$$

to determine values of the perfect-gas heat capacity $C_{p,m}^{pg}$, through the relation

$$C_{p,m}^{pg}/R = \gamma_0/(\gamma_0 - 1), \tag{2}$$

and second β_a and third γ_a acoustic virial coefficients of the gas. [In Eq. (2), γ_0 is the zero- pressure limit of the heat capacity ratio C_p/C_V.] We report values of the coefficients B and C, of the virial equation of state

$$pV_m/RT = 1 + (B/V_m) + (C/V_m^2) + \cdots, \tag{3}$$

obtained by solution of the second-order differential equations:

$$\beta_a = 2B + 2(\gamma_0 - 1)T\frac{dB}{dT} + \frac{(\gamma_0 - 1)^2}{\gamma_0}T^2\frac{d^2B}{dT^2}, \tag{4}$$

and

$$\Gamma_a = \frac{1 + 2\gamma_0}{\gamma_0}C + \frac{\gamma_0^2 - 1}{\gamma_0}T\frac{dC}{dT} + \frac{(\gamma_0 - 1)^2}{2\gamma_0}T^2\frac{d^2C}{dT^2}, \tag{5}$$

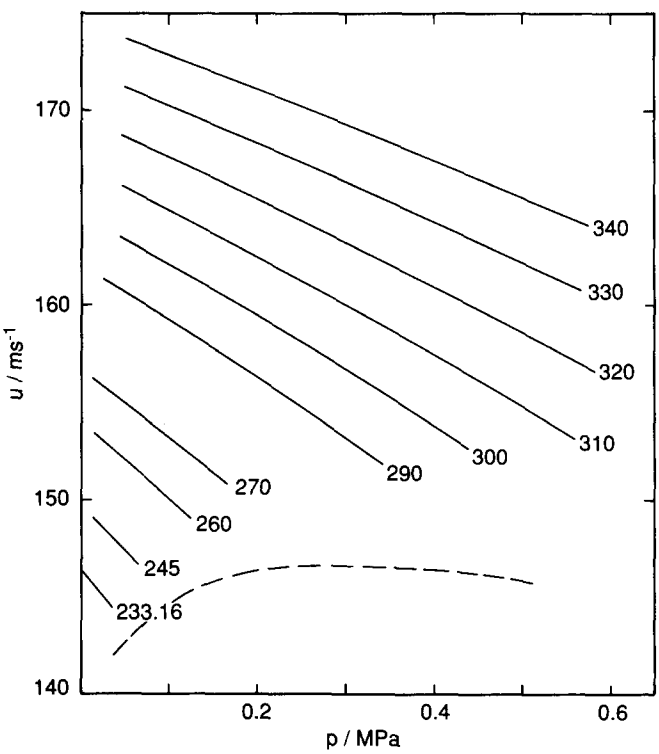

FIG. 1. Speeds of sound u as a function of temperature and pressure p for R134a. The solid curves indicate the pressure range spanned by the data at each temperature. The dashed curve indicates the saturation curve.

[a] Present address: BP Research, Sunbury Research Centre, Sunbury-on-Thames, Middlesex TW16 7LN, U.K.
[b] To whom all correspondence should be addressed.

 0021-9606/90/162741-13$03.00

and where the function Γ_a is given by

$$\Gamma_a = RT\gamma_a + B\beta_a - \frac{\gamma_0 - 1}{\gamma_0} \times \left(B + (2\gamma_0 - 1)T\frac{dB}{dT} + (\gamma_0 - 1)T^2\frac{d^2B}{dT^2}\right)^2. \quad (6)$$

Although the speed-of-sound determines heat capacities and virial coefficients indirectly, the accuracy of the $C^{pg}_{p,m}$ so obtained has been shown to compare favorably with flow calorimetry[4-6] and calculations from spectroscopic data[7-9] while the imprecision of B and C is significantly smaller than that obtained from most conventional $p(V_m,T)$ measurements.[4-9] The values of $B(T)$ deduced from the present speed-of-sound data near $T/T_c = 0.9$ are consistent with the values obtained by Weber[3] from highly accurate $p(V_m,T)$ data. The values of $C(T)$ are not. We cannot explain this discrepancy.

Careful $p(V_m,T)$ measurements can yield accurate virial coefficients at high reduced temperatures; however, such measurements are subject to systematic errors at low reduced temperatures from gas adsorption. In contrast with $p(V_m,T)$ measurements, the speed of sound is independent of the amount of substance and the speed-of-sound data appear to be free from errors related to adsorption. However, our apparatus displayed effects attributed to adsorption of R134a by elastomer O-rings. (See Sec. II F.)

In the present work, the accuracy of the determination of $u(p,T)$ for R134a was approximately $\pm 0.01\%$ and the accuracy of $\gamma_0(T)$ was approximately $\pm 0.1\%$. In both cases instrumental errors were negligible in comparison with our limited ability to characterize and maintain the purity of the gas samples. However, this work does exploit the full precision of the spherical acoustic resonator method of measuring $u(p,T)$ to obtain accurate values of $\beta_a(T)$ for R134a.

II. APPARATUS, MATERIALS, AND PROCEDURES

The acoustic apparatus was designed to rapidly acquire high-quality speed-of-sound data at pressures up to 2 MPa. This objective implies that the apparatus should have: (i) a small gas volume; (ii) good thermal coupling to a thermostat; and (iii) mechanical strength to safely contain the gas. A cross section of the acoustic apparatus is shown in Fig. 2. It was comprised of a spherical shell (the resonator) with an internal volume of $\sim 1/8\ \ell$. The shell was not a pressure vessel; instead, it was surrounded by a heavy-walled aluminum pressure vessel which, in turn, was immersed in a well-stirred thermostatted liquid.

A. The resonator

Spherical acoustic resonators have been developed in recent years as highly precise and accurate tools for measuring the speed of sound in gases.[4-16] Moldover *et al.*[14] demonstrated the strength of the technique by determining the universal gas constant R with a fractional error of 1.7 ppm (parts per million). Using spherical resonators, reliable speeds of sound u have been obtained for a variety of gases near and well below[9,16] room temperature with relative ease.

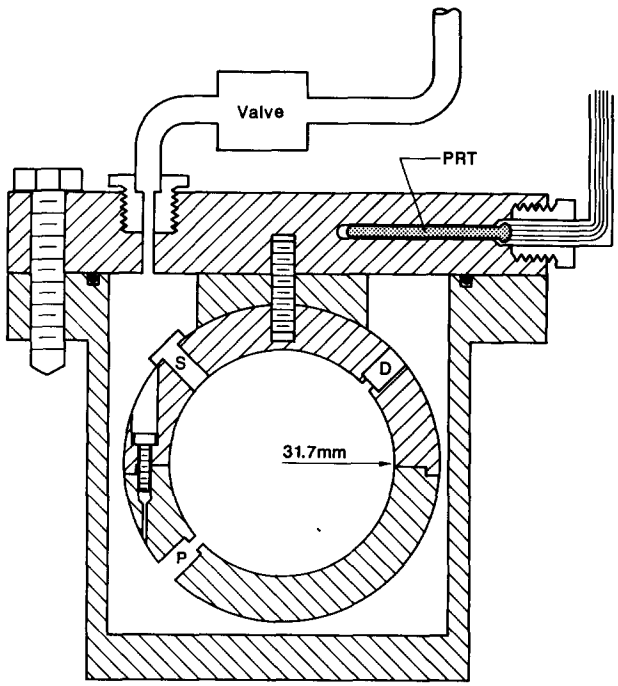

FIG. 2. Cross section through the acoustic apparatus.

A precision of 5 ppm in a $u^2(p)$ isotherm is typical, and virial coefficients and perfect-gas heat capacities can be determined to 0.1% or better. All of these measurements have utilized the low-order radially symmetric modes of such resonators which are designated $(0,n)$ with $n = 2,3,\ldots$. These modes were used because they are nondegenerate and have resonance frequencies that are insensitive to geometric imperfections of the cavity.[17,18] These modes are not subject to viscous dissipation at the wall of the resonator. The low surface-to-volume ratio of a sphere lead to a lower dissipation in the thermal boundary layer than for any other geometry with the same volume. The reduced dissipation contributes significantly to the high precision with which resonance frequencies can be determined.

The present resonator was assembled from two hemispherical shells that had been machined from a single cylindrical bar of yellow brass (65% copper, 35% zinc). The shells had internal radii of 31.7 mm and wall thicknesses of 12.7 mm. The shells were machined at their equators to form an interlocking step, which ensured accurate alignment concentric with the polar axis when they were bolted together. The interior surface of the resonator was polished mechanically to reduce tooling marks. The assembled shell was penetrated by three ports. Two, denoted S and D in Fig. 2, held the acoustic source and detector, respectively. They were located 45° from and coplanar with the "north pole." Port S had been drilled and reamed to a diameter of 6.25 mm. The third port, denoted P in Fig. 2, served to admit gas into the resonator. The innermost portion of this and port D had a diameter of 1 mm and a length $L \approx 3.2$ mm. This arrangement, where L is approximately equal to 1/10 of the cavity's radius, has been shown to reduce spurious resonances that

might interfere with the measurement of the low-order radially symmetric acoustic resonances.[7] The remaining 9.5 mm of port P, extending to the outer surface of the shell, had a diameter of 10 mm.

B. Transducers

The acoustic source was a variant of electrostatic transducers described elsewhere.[13] It was formed by stretching a disk of 12 μm thick polyester sheet around the end of a cylindrical electrode. The active area was 3 mm in diameter. The polyester sheet was held to the electrode with a polytetrfluoroethylene (PTFE) sleeve, which fit snugly in the port S in the resonator. The outer surface of the polyester sheet had a 50 nm thick layer of aluminum on it, which electrically grounded the sheet to the resonator. A potential of 60 V rms was applied to the central cylindrical electrode. When excited in this fashion, the transducer produced sound at twice the frequency of the applied potential. Theoretical models[19] for similar transducers including their annular slots, predict that they perturb the resonance frequencies of the cavity by less than 2 ppm.

The detector was an inexpensive commercially available microphone which had a permanently polarized polyvinylidene fluoride disk as its active element. This transducer was held within its port by a PTFE sleeve. It was acoustically coupled to the spherical cavity through a 15 mm^3 volume and a 1.0 mm diameter wave guide of length 3.2 mm. This arrangement acts as a Helmholtz resonator and its effects on the cavity resonances are small except at the lowest frequencies and lowest pressures.

C. Pressure vessel

The two-piece aluminum pressure vessel was designed using the relevant standards[20] to operate up to 400 K and 2 MPa. (See Fig. 2.) The lower part was machined in one piece from aluminum bar stock. The top plate was machined from the same billet. All threads were appropriately undercut, and sharp corners were removed to reduce concentration of stress in these components. Two coaxial electrical lead throughs rated for 350 K and 10 MPa, were sealed into the top plate using PTFE tape and tapered threads. The pressure vessel was sealed with a Viton[21] elastomer O-ring which did adsorb R134a leading to the problems discussed in Sec. II F. Virtual leaks within the pressure vessel were minimized. All threaded components were relieved to facilitate evacuation of the vessel.

As shown in Fig. 2, the resonator was suspended from the top plate of the pressure vessel by a threaded rod. Excellent thermal contact between the resonator and the thermostatted bath surrounding the pressure vessel was achieved via an aluminum transition piece machined to closely match the external radius of the sphere. Unfortunately, the transition piece was also effective in coupling vibrations from the bath to the resonator. The undesired coupling was reduced to an acceptable level by inserting washers cut from 50 μm thick shim stock between the resonator and the transition piece.

D. Temperature and pressure measurements

The apparatus, including the valve used to seal the gas sample, was suspended inside a stirred fluid bath which was thermostatted to 1 mK. The top plate of the pressure vessel was machined to accept a capsule platinum resistance thermometer, denoted PRT in Fig. 2. The thermometer was never in direct contact with either the pressurized gas or the thermostat fluid. Thermal coupling between the pressure vessel and the thermometer was enhanced with vacuum grease. The temperature of the sample was inferred from the capsule thermometer (Leeds and Northrup,[21] serial number 1818362) and are reported on IPTS-68. The stability of the thermometer was regularly checked in a triple point of water cell. The thermometer, resistance bridge, and the thermal environment of the apparatus were exactly the same during the calibration measurements with argon and during the speed-of-sound measurements in R134a. Consequently, any errors that may have resulted from small temperature gradients remaining in the bath or other aspects of thermometry were compensated to a high degree.

Pressures were measured with a fused-quartz bourdon-tube differential pressure gauge (model no. 6000-801-1, Ruska Instrument Corporation[21]). The manufacturer's calibration data indicated that the gauge had a full scale range of 1 MPa and was linear to 1×10^{-5}. The zero-pressure indication of the gauge varied up to 50 Pa between checks. The reference side of the gauge was continuously evacuated by a mechanical vacuum pump and monitored with a thermocouple vacuum gauge. The R134a sample was separated from the bourdon-tube gauge by a differential pressure transducer (Validyne[21] model DP15TL, serial number 60293), which was operated as a null instrument. The pressure difference sustained by this transducer was always <2 kPa and typically <0.2 kPa. The transducer's span was 8 kPa and, when calibrated against the bourdon-tube gauge, was found to be linear to 9 Pa. The zero indication of the differential pressure transducer was measured as a function of the pressure. It was always less than 30 Pa and could be represented to 3 Pa with a linear expression.

E. Purity of gases

The R134a was manufactured by E. I. Du Pont De Nemours & Co.[21] The manufacturer provided the analysis for the first four compounds listed in Table I, however, no information was provided concerning water and air impurities. Dr. T. Bruno of the Properties of Fluids Group of NIST conducted a chromatographic analysis[22] of the material as supplied. He reported 215 ppm of water. Before we used the R134a, a gas phase sample was slowly distilled from the suppliers cylinder, which contained a two-phase sample, to a small stainless-steel ampoule, fitted with a bellows valve. The gas phase sample was then further dried by passing slowly over a grade 4A molecular sieve, previously baked at 550 K for 24 h. The sample was collected downstream from the drier where it was finally degassed by vacuum sublimation using a liquid-nitrogen cooled finger. This process required repeated cycles of freezing, evacuation, and melting. The acoustic apparatus was then filled by allowing the sample to warm slowly from 77 K until the required pressure was reached. During the course of a set of measurements, the pressure was reduced in decrements by condensation of

TABLE I. Substance i and mole fraction x_i of each component in the R134a sample.

i	x_i
1,1,1,2-Tetrafluoroethane	balance
Pentafluoroethane	0.000 156
1,1,1-Trifluoroethane	0.000 159
1-Chloro-2,2-difluoroethane	0.000 150
H_2O	0.000 105
Air	0.000 005

R134a back into the stainless-steel ampoule. Subsequently, this material was reused after further degassing and drying. A single sample was recovered from the resonator after ten isotherms had been studied and before the repetition of the 300 and 310 K isotherms. The analysis showed that the water and air content were 105 and 5 ppm, respectively. These results are listed in Table I and were used to calculate the molar mass of the sample required to deduce $C^{pg}_{p,m}$ from the speed of sound.

The argon used in the calibration measurements was taken from the same cylinder that supplied the working gas in the recent redetermination of the universal gas constant.[14] The sample was supplied by Matheson Gas Products[21] (in cylinder 45024T) with a lot assay (E30 000 6D8) indicating upper bounds for the impurities: N_2, O_2, H_2O, and hydrocarbons totaling <4 ppm. Moldover *et al.*[14] determined that the ratio $M/\gamma_0 = 23.968\,68_4$ g/mol for this cylinder of argon and they provided extensive details concerning tests for other possible impurities.

F. Sorption effects

When the pressure vessel was first filled with R134a at a temperature of 290 K and a pressure of 350 kPa, we noted that the pressure decreased slowly and the acoustic resonance frequencies increased slowly, just as if some gas were being removed from the resonator. Ultimately the pressure approached a constant value approximately 1 kPa lower than the initial pressure with an apparent time constant of ~ 7 h. The resonance frequencies changed in a corresponding manner. Subsequently some of the R134a was removed from the pressure vessel. Then, the pressure slowly rose and the frequencies decreased in a corresponding manner. These "memory" effects would have been expected if there had been a volume of 1 cm^3 connected to the pressure vessel through a constriction. No such volume was present; the "memory" effects did not occur when argon was in the apparatus. We speculate that these effects resulted from the large adsorption (or solution) of R134a in the O-ring used to seal the pressure vessel.

In general, the sorption problem was coped with by measuring the resonance frequencies as quickly as possible and by recording the pressure before and after the frequency measurements. Typically, the measurements of the resonance frequencies were completed within 20 min following a pressure change, and much of this interval was spent waiting for the thermal equilibration of the resonator. To check these practices, an especially detailed study of the 290 K isotherm was made. Each of the five or six resonance frequencies measured at each nominal pressure was corrected for the observed pressure drift. Equation (1) was fitted separately to the original data and to the corrected data. The resulting parameters are:

	Corrected	Uncorrected	Difference
$C^{pg}_{p,m}/R$	10.0441 ± 0.0019	10.0461 ± 0.0018	0.0020 ± 0.0026
$\beta_a/(cm^3/mol)$	-809.28 ± 0.56	-808.3 ± 0.47	-0.98 ± 0.73
$\gamma_a/(cm^3/mol\ MPa)$	-133.5 ± 2.5	-137.4 ± 2.1	3.9 ± 3.3

The differences in the fitted parameters are barely significant statistically and they are certainly much smaller than the changes that resulted when the R134a was condensed out of the pressure vessel and redistilled into it.

At 320, 330, and 340 K, the desorption of R134a from the elastomer was so rapid that accurate acoustic measurements could not be made below 100 kPa.

G. Frequency measurements and corrections

Before a series of measurements, the resonator was maintained at 350 K and evacuated until the pressure indicated by a thermocouple gauge in the pumping line had been below 1×10^{-3} Pa for 24 h. The zero of the differential pressure gauge was adjusted and the resonator flushed and filled with R134a or the calibrating gas. On each isotherm, the initial filling was up to the highest pressure to be studied. The resonator was allowed to come to thermal equilibrium and then the valve leading to the pressure vessel was closed.

The resonance frequencies f_{0n} and the half-widths g_{0n} of the radial modes were obtained from measurements of the amplitude and phase of the detected voltage as a function of the frequency of the acoustic source using the methods described in detail elsewhere.[13] Usually, three complex parameters were fitted to the data for each mode. A fourth was included only when it led to a significant reduction in χ^2.

The zero-frequency speeds of sound u were obtained from the measured frequency f_{0n} using

$$u = 2\pi a(f_{0n} - \Delta f_{th} - \Delta f_p - \Delta f_{el})/\nu_{0n}, \qquad (7)$$

where a is the resonator's radius, ν_{0n} is an eigenvalue which is known exactly, and the Δf are small correction terms. This model was developed by Moldover, Mehl, and Greenspan and has been described in detail numerous

times.[4,10,11,13,14,23-25] In Eq. (7) the subscripts th, p, and el refer to terms which take account of the thermal-boundary layer, ports in the resonator's wall, and the elastic response of the shell.

For the present measurements, the thermal-boundary-layer correction is the most important. To implement it for R134a, we used the thermal conductivity data reported by Shanklin *et al.*[26] between 298.15 and 343.15 K. Their data for six dilute-gas measurements had an accuracy of 2% and are represented with a standard deviation of 0.05 mW/(m K) by the correlating expression[27]

$$\kappa/(\mathrm{mW/(m\,K)}) = 29.742 - 0.1796(T/\mathrm{K}) + 426.5\times10^{-6}(T/\mathrm{K})^2. \quad (8)$$

Upon extrapolation to temperatures below the data, the thermal conductivities given by Eq. (8) are larger than those obtained by extrapolation with the rule of Owen and Thodos.[28] ($\kappa = \kappa_0 T^n$, with $n = 1.797$.) The difference increases to 18% of κ at our lowest temperature, 233 K. We took the difference as a measure of the uncertainty associated with the extrapolation and concluded that the correction to the resonance frequencies was uncertain by ~9 ppm in the worst case. If the results at 233 K were analyzed using κ from the Owen and Thodos rule, the values of γ_0, β_a, and γ_a, would differ from those listed in Table III by no more than 1.1 times the combined standard deviations, a statistically insignificant amount. At higher temperatures the effects of the uncertainty in κ are much smaller.

All the remaining corrections are very small. They were made for the sake of completeness and to search for possible inconsistencies in the data.

The thermal-boundary-layer correction, includes a small term to account for the temperature-jump effect[25] and it was made assuming that the thermal accommodation coefficient was unity. The shell motion correction required knowledge of the shell's compliance, density, and breathing resonance. The compliance was calculated to be 99.6 TPa^{-1} using published values of Poisson's ratio and Young's modulus.[29] The shell's density was measured and the breathing resonance was calculated to be 27.3 kHz. $\Delta f_{\mathrm{el}}/f$ was never greater than 9 ppm. The theoretical corrections for the gas-inlet port and the detector coupling tube $\Delta f_p/f$ never exceeded 15 ppm and the uncertainty in the correction is much smaller. The detector and its coupling tube form a Helmholtz resonator but, as noted elsewhere,[13] leakage conductance is important and difficult to estimate. The uncertainty in these corrections is on the order of 10 ppm.

The shear viscosity, required to determine the absorption throughout the bulk of the gas and to correct for openings in the resonator wall was calculated from the modified Eucken equation:[30]

$$\eta = \kappa M/(1.77 + 1.33C_{V,m}/R), \quad (9)$$

using the thermal conductivities from Eq. (8). The heat capacity and density were calculated, correct to the second virial coefficient which was obtained from a preliminary analysis of the results. Small corrections were applied to correct all values of u to the stated temperatures.

III. CALIBRATION OF THE RESONATOR WITH ARGON

The performance of the resonator was evaluated and its radius was determined from acoustic measurements made while the resonator was filled with argon. These measurements were made on isotherms at 233.15, 282, 300, 320, 330, and 350 K. The resonance frequencies and half-widths were measured for the four lowest-frequency radially symmetric modes on each isotherm. At least six pressures were used with values near 700, 575, 450, 325, 200, and 75 kPa on each isotherm.

In order to calculate the half-widths and to correct the frequencies, we used the thermophysical properties of argon calculated from the Hartree–Fock plus damped dispersion (HFDB-2) interatomic potential-energy function of Aziz and Slaman.[31] Thermal conductivities were calculated correct to second order in the Kihara approximation scheme. These values were compared with experiment and found to be more than adequate for our needs. The second virial coefficients were calculated correct to the second quantum correction using the HFDB-2 potential. For the (0,3) mode, $\Delta f_{\mathrm{th}}/f_{0n}$ varied from 75 ppm at 233.16 K and 733 kPa to 464 ppm at 350 K and 34 kPa. The shell correction never contributed more than 26 ppm.

A preliminary examination of both the frequency and half-width data showed that the (0,5) mode was perturbed by the breathing resonance of the shell, particularly at the highest temperatures and pressures. For the (0,2) mode, the fractional excess half-width, defined by the relation

$$\Delta g/f_{0n} = (g_{0n} - g_{th} - g_t - g_b)/f_{0n}, \quad (10)$$

ranged from 30 to 45 ppm at all temperatures and pressures. This was larger than expected from prior experience with similar resonators[4,7,11,13,23] and larger than the excess half-widths of the (0,3) and (0,4) modes in the present resonator. (Depending upon the state, they ranged from 10 to 20 ppm.) Furthermore, at low pressures the frequency of the (0,2) mode was typically 20 ppm below that expected from the mean of the other modes. Perhaps these observations could be explained by improved modeling of the thermal link or the Helmholtz resonance associated with the detector transducer.

For calibration purposes, we used the frequency measurements for the (0,3) and (0,4) modes for all state points and the (0,2) mode at higher pressures. After correcting the frequencies, Eq. (7) was used to calculate u/a for each mode and the resulting values were averaged to obtain values of $\langle u\rangle/a$ with standard deviations in the range 2 to 8 ppm.

A modified form of Eq. (1) having six parameters was fit to the values of $\langle u(p,T)\rangle/a(T)$ at all 40 state points. Three parameters accounted for the temperature-dependent average radius of the shell $a(T)$. The fourth parameter was added to the values of β_a calculated from the HFDB-2 potential to allow for imperfect agreement between the calculation and the data. The remaining two parameters account for a temperature-dependent γ_a. This analysis gave

$$\frac{(u/a)}{\mathrm{s}^{-1}} = \left[\frac{RT\gamma_0}{M} + \frac{\gamma_0}{M}\left[\beta_a(\mathrm{calc}) + 0.196\right]\frac{p}{\mathrm{MPa}} + (52.78 - 0.176t)\left(\frac{p}{\mathrm{MPa}}\right)^2\right]^{1/2}\Big/a(T), \quad (11a)$$

where

$$a(T) = 3.177\,624\ \text{cm} \times (1 + 18.8 \times 10^{-6} t + 7.897 \times 10^{-9} t^2) \quad (11b)$$

and

$$t \equiv (T/\text{K} - 273.15). \quad (11c)$$

The fractional standard deviation was 3.4 ppm. The experimental results are shown as deviations from Eq. (11) in Fig. 3. In Eq. (11), β_a(calc) is in cm^3/mol, $R = 8.314\,471$ J/K mol), and $M/\gamma_0 = 0.023\,968\,68_4$ kg/mol.

The present argon data can be compared with data from the literature. To do so, Eq. (1) was fitted to the argon data on each isotherm separately. The fractional standard deviations were barely less than those obtained by fitting the surface, Eq. (11). In Fig. 4, the resulting values of β_a are shown as deviations from those calculated from the HFDB-2 potential which was derived without reference to any of these data. The present values of β_a average only 0.2 cm^3/mol higher than the smooth function of temperature obtained from the HFDB-2 potential. Recent values of β_a obtained by other workers are also shown in Fig. 4. The individual values of β_a have statistical imprecisions which are considerably less than the scatter at each temperature; however, the various values were determined from measurements in different apparatus and in different pressure ranges using various orders of fit. Overall, the agreement is remarkable.

A final test of the calibration procedure is a comparison of the linear thermal expansivity of the resonator determined from Eq. (11) with that obtained from the literature.[32] They differed by 0.7%.

From the calibration procedure, the average radius of the resonator is known with a standard deviation of 0.3 μm. Uncertainties in a contribute less than 0.0001 R to the error in $C^{\text{pg}}_{p,m}$ of R134a. One year after these calibration measurements, the transducers were replaced and the calibration was checked at 300 K. The resonance frequencies increased an average of 13 ppm, indicating that the dimensional stability of the resonator is satisfactory.

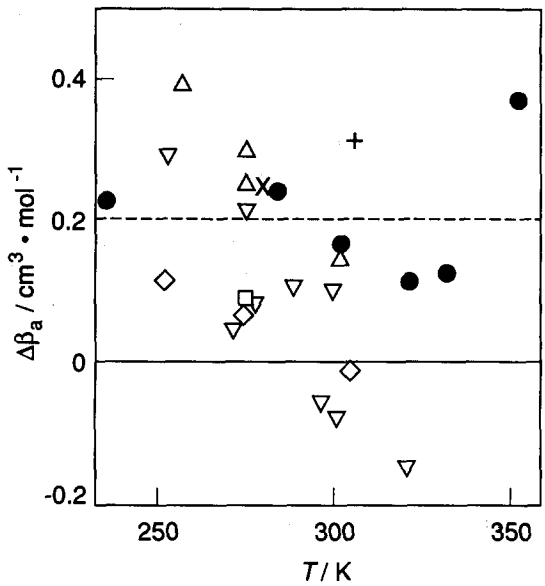

FIG. 4. Deviations $\Delta\beta_a = \beta_a - \beta_a$(calc) of various experimental second acoustic virial coefficients of argon from those calculated from the HFDB-2 potential.– – –, this work, Eq. (11); ●, this work, separate fits to each isotherm; △, Ref. 7; ▽ Ref. 4; ◇, Ref. 16; □, Ref. 25; +, Ref. 15; ×, Ref. 14.

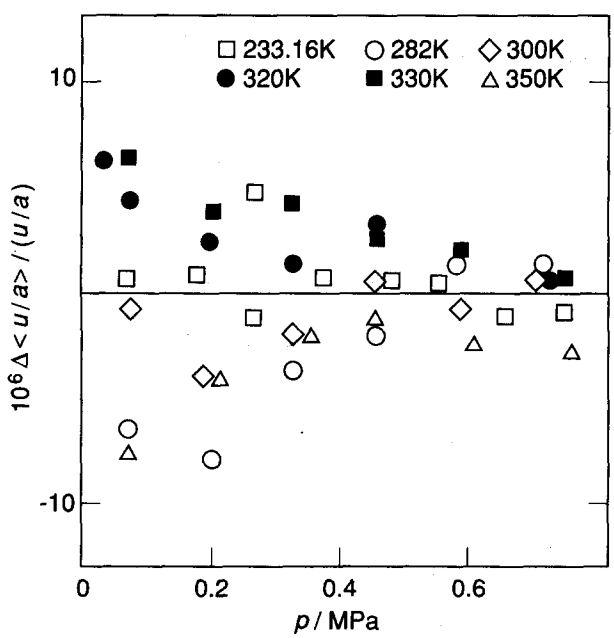

FIG. 3. Deviations $\Delta\langle u/a\rangle$ of the argon calibration data from the surface $u(p,T)/a(T)$ defined by Eq. (11). The deviations are the measured values minus the calculated values, scaled by $10^6/\langle u/a\rangle$.

IV. RESULTS FOR R134A

A. Speed-of-sound data for R134a

The resonance frequency measurements for R134a were made along ten isotherms between 233.16 and 340 K. A portion of the gas was withdrawn for analysis and then the measurements on the isotherms at 300 and 310 K were repeated. The maximum pressure along the isotherms below 310 K was restricted to 0.6 of the vapor pressure, to avoid the known effects of precondensation.[23] Of the other isotherms, the greatest pressure was about 580 kPa, which is near the vapor pressure of R134a at room temperature.

The speeds of sound were obtained from the corrected resonance frequencies together with the values of the resonator's radius determined from the measurements with argon. Consistent speed-of-sound results, at a level of 8 ppm, were obtained with R134a using the five lowest-frequency radially symmetric modes under most conditions. At 233 and 245 K, measurements were made using only the (0,3), (0,4), and (0,5) modes to save time.

Table II lists mean speeds of sound at each temperature and pressure, together with fractional standard deviations and the number of resonant modes from which they were determined.

TABLE II. Mean values of the speed of sound u with fractional standard deviations $\sigma = 10^6 s(u/u)$ determined from N radial modes, and deviations $\delta = 10^6[\langle u^2\rangle - u^2(\text{calc})]/u^2(\text{calc})$ from Eq. (1) with three terms at temperatures T and pressures p in R134a.

T (K)	p (kPa)	$\langle u\rangle$ (m/s)	σ (ppm)	N	δ (ppm)	p (kPa)	$\langle u\rangle$ (m/s)	σ (ppm)	N	δ (ppm)
233.160	37.511	144.4091	2.4	3	a	20.229	145.3782	1.0	3	−2.1
	32.792	144.6775	1.8	3	−2.1	16.209	145.6000	0.4	3	−0.6
	29.772	144.8470	0.8	3	2.4	12.931	145.7798	0.1	3	−1.9
	26.656	145.0216	1.0	3	3.6	9.621	145.9604	0.4	3	−5.6
	23.830	145.1792	1.1	3	6.3	5.610	146.1792	1.3	3	5.0
245.000	71.368	146.4530	3.2	3	−8.9	29.674	148.4770	4.9	4	1.0
	64.067	146.8157	3.0	3	3.8	23.201	148.7816	5.5	4	−3.9
	56.513	147.1858	2.6	3	−6.8	15.936	149.1202	4.1	4	−15.2
	50.005	147.5047	6.7	4	20.3	6.867	149.5417	2.9	4	12.6
	36.886	148.1338	6.4	4	−5.9					
260.000	129.031	148.8391	6.5	5	−7.3	59.739	151.6970	8.1	5	4.7
	115.220	149.4247	6.6	5	11.6	45.134	152.2750	10.0	5	−8.8
	100.345	150.0439	6.8	5	−11.5	29.953	152.8687	6.3	4	−5.6
	85.985	150.6375	7.1	5	18.6	18.774	153.3015	4.4	4	9.0
	72.336	151.1901	7.4	5	−10.1					
270.000	170.427	150.6168	5.8	5	a	80.473	153.9413	7.2	5	−8.0
	153.467	151.2616	6.9	5	a	63.229	154.5548	7.3	5	11.3
	138.143	151.8377	7.1	5	−6.4	48.764	155.0609	8.9	5	−6.2
	118.384	152.5696	7.1	5	8.4	29.871	155.7147	2.4	4	−18.5
	96.088	153.3813	7.1	5	3.7	11.942	156.3300	3.1	4	10.4
290.000	345.136	151.7079	3.6	5	a	100.874	159.1906	6.8	6	−3.2
	299.377	153.1982	4.6	5	a	101.065	159.1854	7.0	6	0.8
	250.981	154.7233	9.5	6	a	50.686	160.6068	12.0	6	−3.7
	196.130	156.4011	7.9	6	−2.4	22.766	161.3799	5.4	4	4.3
	149.117	157.7954	6.1	6	5.6					
300.000	403.387	153.7566	6.8	5	a	175.047	160.1551	8.1	6	5.9
	321.994	156.1233	12.1	6	a	124.498	161.4762	8.5	5	−11.6
	274.812	157.4529	11.2	6	−3.4	49.814	163.3764	8.2	5	3.5
	225.516	158.8038	9.5	6	4.3					
300.000	437.641	152.6959	3.8	5	a	180.858	159.9748	6.3	5	5.2
	374.840	154.5687	5.5	5	a	120.093	161.5655	6.1	5	−4.8
	295.748	156.8393	6.8	5	a	57.432	163.1624	7.5	5	1.5
	238.137	158.4338	5.4	5	−1.8					
310.000	559.156	153.1884	5.2	5	a	247.841	161.3421	9.0	5	15.9
	489.949	155.1046	5.9	5	a	146.995	163.7571	3.9	5	−15.3
	420.274	156.9710	9.0	5	a	49.147	166.0165	6.7	5	5.0
	343.718	158.9529	9.6	5	−5.7					
310.000	505.464	154.6632	10.8	5	a	239.324	161.5370	2.3	5	−3.8
	400.880	157.4670	4.7	5	a	159.519	163.4478	2.7	5	12.8
	350.710	158.7620	6.9	5	a	90.592	165.0520	5.6	5	−14.1
	299.064	160.0653	3.5	5	a	27.784	166.4838	10.8	5	5.1
320.000	585.584	156.5344	5.4	5	a	298.918	163.2765	10.1	5	14.6
	492.856	158.7970	7.9	5	a	197.056	165.5071	9.1	5	−14.2
	398.227	161.0226	9.9	5	−5.1	98.258	167.6028	5.7	5	4.7
330.000	565.988	160.7755	5.3	5	a	299.346	166.3429	4.6	4	17.8
	476.423	162.6991	7.5	5	−1.4	197.918	168.3460	8.0	5	−15.7
	395.905	164.3778	10.7	5	−2.6	98.974	170.2507	5.5	5	5.5
340.000	575.184	164.0881	5.2	5	a	380.355	167.7818	8.4	5	4.1
	573.915	164.1159	5.7	5	−3.5	298.693	169.2754	8.4	5	−7.5
	474.894	166.0137	8.1	5	5.2	102.000	172.7558	5.5	5	1.6

[a] Pressure omitted from analysis.

B. Truncated pressure expansion

For R134a, all measurements of the resonance frequencies were considered for the regression analysis using Eq. (1) to determine $\gamma_0(T)$, $\beta_a(T)$, and $\gamma_a(T)$. Below 270 K and at 340 K, three terms were sufficient to fit the data to within experimental error. Between 270 and 330 K four terms were required to adequately accommodate the data.

The highest-order term fitted to Eq. (1) is subject to systematic error because the virial expansion is truncated. Thus, the phrase "apparent γ_a" is properly used to describe the value of γ_a resulting from a three-term fit to Eq. (1). To avoid possibly meaningless comparisons between values of γ_a resulting from three-term fits and γ_a resulting from four-term fits, we omitted the highest-pressure data on the iso-

therms from 270 to 330 K and used only three-term fits. (The data that were omitted from the fit are noted in Table II.) At 233 K the data at the highest pressure was omitted because it was clearly perturbed by precondensation.[23]

The values of $C_{p,m}^{pg}$, β_a, and γ_a resulting from three-term fits to the R134a data are listed in Table III. Figure 5 displays the differences between the data and the three-term fit for a typical isotherm at 260 K. At each pressure, the differences between the data and the fit are comparable to the differences between the results for the five modes studied. Thus, additional pressure dependent terms could not improve the fit for this isotherm.

If the highest pressure data on the isotherms between 270 and 330 K had been used in the three-term fits, the values of $C_{p,m}^{pg}$ would have changed by 0.008 R (0.09%), an amount within one combined standard deviation of the fits. At 320 K (the worst case), β_a would have changed by 3 cm^3/mol (0.5%). The change in β_a at 270 K would have been 1.4 cm^3/mol (0.1%).

If we had used all of the data and four-term fits, the values of $C_{p,m}^{pg}$ would have changed by 0.008 R, again, an amount within one combined standard deviation. Typically, the change in β_a would have been 3 cm^3/mol (about 0.4%), within two combined standard deviations.

These changes resulting from alternative fitting procedures are measures of the systematic errors arising from truncation of the infinite virial series.

Although the pressure is one of the quantities measured, we considered fitting a power series in the amount-of-substance density to the speed-of-sound data. The same number of terms were required to accommodate the results. In all cases the resulting values of β_a and $C_{p,m}^{pg}$ agreed with the pressure-explicit expansion within the combined standard deviation.

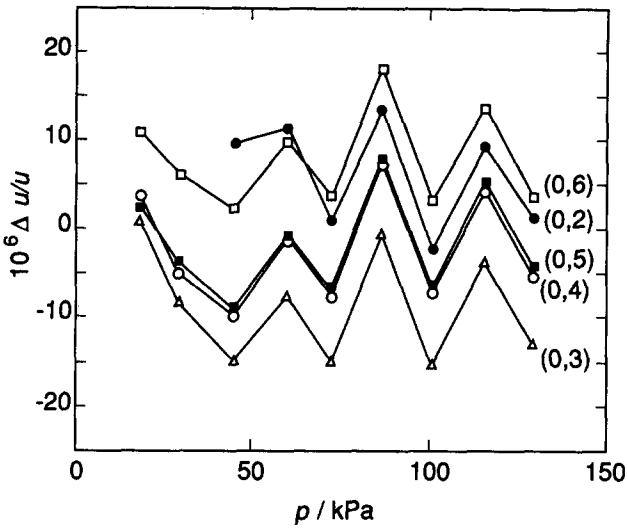

FIG. 5. Fractional deviations $\Delta u/u = [u - u(\text{calc})]/u$, for individual modes in R134a at 260 K, from Eq. (1) with coefficients from Table III. The lines are drawn to guide the eye.

C. Repeatability of the data

After a complete set of $u(p,T)$ data was acquired for R134a, the isotherms at 300 and 310 K were remeasured. These repeated isotherms yielded values of $u(p,T)$ that were approximately 0.01% smaller than the first values. The 300 K isotherm showed the larger changes:

	measurement 1	measurement 2	difference
$C_{p,m}^{pg}/R$	10.2298 ± 0.0029	10.2535 ± 0.0028	−0.0237 ± 0.0040
β_a (cm^3/mol)	−740.61 ± 0.52	−742.18 ± 0.58	1.57 ± 0.78
γ_a/(cm^3/mol Pa)	−113.6 ± 1.6	−110.5 ± 1.9	−3.1 ± 2.5

TABLE III. Perfect-gas heat capacities, second and third acoustic virial coefficients, and standard deviations s obtained by analysis of N modes in R134a. Uncertainties are one standard deviation.

T/K	N	$C_{p,m}^{pg}/R$	β_a/(cm^3/mol)	γ_a/(cm^3/(mol MPa))	$10^6 s(u^2)/u^2$
233.16	27	8.733 75 ± 0.000 57	−1424.0 ± 0.9	−710.5 ± 24	4.3
245.00	33	9.012 84 ± 0.001 25	−1239.8 ± 1.1	−578.6 ± 13.3	13.9
260.00	43	9.362 92 ± 0.001 81	−1059.3 ± 0.8	−370.8 ± 4.9	16.6
270.00	38	9.584 33 ± 0.001 49	−964.60 ± 0.59	−250.5 ± 3.7	15.5
290.00	34	10.046 1 ± 0.001 8	−808.30 ± 0.47	−137.4 ± 2.1	15.1
300.00	28	10.229 8 ± 0.002 9	−740.61 ± 0.52	−113.6 ± 1.6	17.9
300.00[a]	20	10.253 5 ± 0.002 8	−742.18 ± 0.58	−110.5 ± 1.9	12.5
310.00	20	10.472 6 ± 0.002 8	−685.46 ± 0.44	−85.5 ± 1.1	18.3
310.00[a]	20	10.487 5 ± 0.002 2	−688.01 ± 0.51	−74.5 ± 1.9	16.1
320.00	20	10.681 5 ± 0.004 9	−632.96 ± 0.59	−67.7 ± 1.2	19.4
330.00	24	10.858 9 ± 0.003 8	−588.56 ± 0.39	−49.5 ± 0.7	17.3
340.00	25	11.103 1 ± 0.002 6	−546.05 ± 0.22	−39.2 ± 0.3	13.8

[a] Repeat isotherm.

The differences in β_a and γ_a are within two combined standard deviations; however, the difference in $C^{pg}_{p,m}$ is six combined standard deviations. The heat capacity is extremely sensitive to the concentration of impurities with high speeds of sound such as water and air. A decrease in the mole fraction of water by 0.000 28 would cause the increase in $C^{pg}_{p,m}$ that was observed. (A mole fraction 0.000 105 of water was observed between the speed-of-sound measurements. See Table I.) Such a change is larger than we would expect; however, it cannot be ruled out by the measurements that were made.

D. Excess half-widths

The excess half-widths $\Delta g_{0,n}$ were analyzed to test the consistency of the measurements and to obtain estimates of the vibrational relaxation time τ. The expression

$$\Delta g_{0,n} = [(\gamma - 1)A\pi f^2_{0,n}/\rho]b_b + f_{0,n}b_r + b_{\rm th}(f_{0,n}/\rho)^{1/2} \quad (12)$$

was used. In Eq. (12), A is defined as $C_{\rm vib}/C_{p,m}$, where $C_{\rm vib}$ is $(C^{pg}_{p,m} - 4R)$, the vibrational contribution to the heat capacity, ρ is the mass density, $b_b = \tau\rho$, and b_r is an empirical factor that accounts for the unexplained loss mechanisms. In this analysis b_r was set equal to the value obtained from the measurements with argon, and as expected only the term b_b was significant. At the pressure 101.325 kPa, the vibrational relaxation times were 55 ns at 233 K, 90 ns at 270 K, and 72 ns at 340 K. The term $b_{\rm th}$ was not significant for any isotherm and confirms that Eq. (8) gave κ with sufficient accuracy for our purposes.

We observed that the (0,6) mode in R134a had an exceptionally large value of $\Delta g/f$ at the highest pressures. Then $\Delta g/f$ was about a factor of 4 greater for the (0,6) mode than for the other modes. A similar discrepancy has been observed in two other resonators[7,25] and was attributed to strong coupling between the (0,6) mode and a mechanical resonance of the shell.

V. ANALYSIS

A. Molar perfect-gas heat capacity at constant pressure

The heat capacities of Table III may be represented by

$$C^{pg}_{p,m}/R = 2.2540 + 0.0317(T/{\rm K}) - 16.8\times10^{-6}(T/{\rm K})^2 \quad (13)$$

with a standard deviation of 0.0081 R. The results are shown as deviations from Eq. (13) in Fig. 6. As with other substances studied using this technique, the scatter in the data greatly exceeds the imprecision in fitting any single isotherm. We suspect that small variations in the quantity of water and/or air is responsible. We are not aware of other measurements of the heat capacity of R134a that could be compared with the present data.

Figure 6 also displays the calculations of Chen *et al.*[33] and of Basu and Wilson[34] which are based on spectroscopic information. We take the differences between the calculations as a measure of the uncertainty in calculating $C^{pg}_{p,m}$ for a molecule as complicated as R134a. The calculated values of $C^{pg}_{p,m}$ exceed the experimental values by 1.2% to 2.8%,

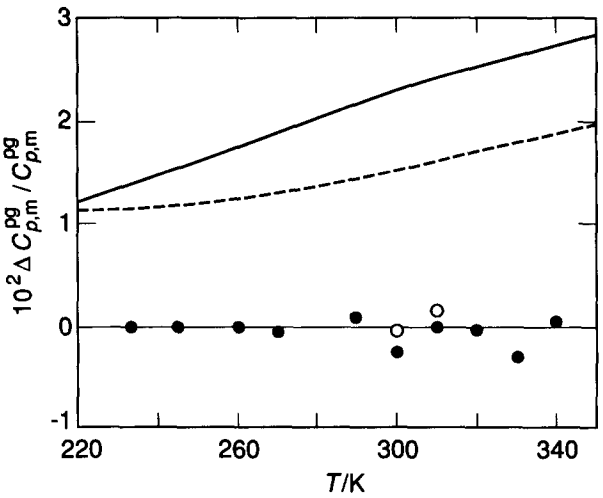

FIG. 6. Fractional deviations $\Delta C^{pg}_{p,m}/C^{pg}_{p,m} = [C^{pg}_{p,m} - C^{pg}_{p,m}({\rm calc})]/C^{pg}_{p,m}$ of perfect-gas heat capacities of R134a from Eq. (13). ●, this work from Table I, first sample; ○, this work, repeat isotherms;—, Ref. 34; ---, Ref. 33.

amounts that exceed the worst case irreproducibility of the experiments by factors of 5–12.

B. Determination of $B(T)$ by integration

We now consider the calculation procedure for calculating the low-density $p(V_m,T)$ surface from our results. Formally, the second virial coefficient B can be determined from the experimental information by numerically integrating the differential equation (4). Integration of this equation with specified boundary conditions has been demonstrated by Bruch[35] for ^{4}He, and by Mehl and Moldover using their precise experimental β_a for ethylene.[8] In the latter case the accuracy of the results was confirmed by comparison with precise $p(V_m,T)$ results. However, integration favors the use of at least one initial condition near the lowest temperature.[36] Appropriate data were not available for R134a, thus integration was not attempted.

The alternative we adopted assumes explicit functional forms for $B(T)$ and uses Eq. (4) to calculate $\beta_a(T)$ which is then compared with the speed-of-sound results. This procedure is similar to that described in detail by Ewing *et al.*[4–7,12] No explicit account is taken of the integration constants required for the general solution to the differential equation, however, Boyd and Mountain argued that this method does, in fact, take implicit account of the homogeneous solution.[37]

C. Model square-well potential for $B(T)$

A model square-well intermolecular potential has been used with success to analyze speed of sound for other thermodynamic information, particularly by Ewing *et al.*[4–7,9,12] For the second virial coefficient, the square-well model leads[38] to the simple expression

$$B(T) = b_0[1 - (r^3 - 1)\Delta], \quad (14a)$$

with

$$\Delta = \exp(\epsilon/kT) - 1. \tag{14b}$$

In Eqs. (14), there are three parameters to be fit to the data: the co-volume b_0, the scaled well depth ϵ/k, and the ratio of the radius of the well to the radius of the hard core r. From Eq. (4) the corresponding expression for β_a is

$$\beta_a/2b_0 = r^3 + \left[-1 + \frac{(\gamma_0 - 1)}{\gamma_0}\frac{\epsilon}{kT} - \frac{(\gamma_0 - 1)^2}{2\gamma_0}\left(\frac{\epsilon}{kT}\right)^2\right](r^3 - 1)\exp(\epsilon/kT) .$$

For R134a, this model led to a very good representation of both our results for $\beta_a(T)$ and Weber's results[3,39] for $B(T)$. However, the same parameters that represented $\beta_a(T)$ failed to represent $\gamma_a(T)$. Presumably this failure results from the large dipole moment of R134a and secondarily from the fact that the R134a molecule is not a hard sphere and from three-body interactions.

The three parameters in the square-well model were determined by a weighted nonlinear fit to the values $\beta_a(T)$ listed in Table III as well as the values of $B(T)$ obtained by Weber. Both sets of data are shown in the upper part of Fig. 7. These values were weighted inversely as the square of an "estimated standard deviation" σ_{est} which was chosen to be $0.002\times\beta_a$ or $0.002\times B$, as appropriate. For the β_a data, σ_{est} is roughly a factor of 3 times the standard deviations of β_a obtained from the fits to the various isotherms and listed in Table III. The factor of 3 accounts for the *irreproducibility* of the isotherms evident upon repetition. For the B data, σ_{est} is an estimate of the *accuracy* of Weber's values of B. His values of $B(T)$ are much smoother; however, Weber[39] investigated the effects of truncating virial expansion and concluded that the systematic uncertainties in $B(T)$ are on the order of 0.6 cm^3/mol near 368 K. In fitting the square-well model, Eq. (13) was used to represent the experimental values of $\gamma_0(T)$ required to calculate $\beta_a(T)$. The regression led to the parmeters: $b_0 = 79.95$ cm^3/mol, $\epsilon/k = 601.6$ K, and $r = 1.2807$; and the standard deviation of the fit was 1.5 cm^3/mol. The lower part of Fig. 7 shows the differences between the data and the values calculated from Eqs. (4), (13), and (14). Both $\beta_a(T)$ and $B(T)$ are fitted with extraordinary high precision over the wide range of temperature $0.62 \leqslant T/T_c \leqslant 1.13$.

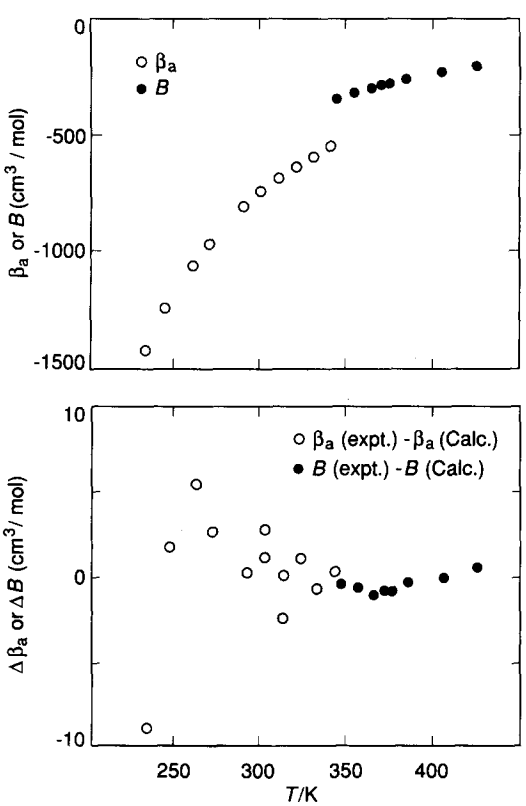

FIG. 7. Top: Measurements of the second virial coefficient B and the second acoustic virial coefficient β_a as a function of temperature. Bottom: Deviations of the measurements from the model square-well potential with the parameters: $b_0 = 79.95$ cm^3/mol; $\epsilon/k = 601.6$ K; and $r = 1.2807$; and γ_0 calculated from Eqs. (2) and (13).

On Fig. 7, there is no discontinuity in the deviation plot near 340 K, the temperature where both β_a and B were measured. This demonstrates the remarkable consistency of the present $u(p,T)$ data with Weber's high-quality $p(V_m,T)$ data. Near 340 K, the numerical values $\beta_a(T)$ are approximately twice the values $B(T)$ and the deviations of β_a from the fit are approximately twice those in B. These observations are similar to the findings of Ewing *et al.*[4-7,9] who measured $u(p,T)$ for alkanes using a spherical acoustic resonator and examined their results with model square-well potentials.

The acoustic determination of $\beta_a(T)$ exploits the precision of the measurements of $u(p,T)$ on isotherms. Problems caused by impurities are less significant in the determination of $\beta_a(T)$ than in the determination of $C^{pg}_{p,m}(T)$ for two reasons. First, the acceptable fractional errors in $\beta_a(T)$ or $B(T)$ are usually an order of magnitude larger than the errors in $C^{pg}_{p,m}(T)$, and second, the relation between $C^{pg}_{p,m}$ and u amplifies the errors in u by a factor of $1/(\gamma_0 - 1)$.

There are two features that contributed to the success of this method of calculating B from β_a. First, the second virial coefficient is relatively insensitive to the detailed shape of the potential energy function, so that a crude approximations to the true potential can represent B with sufficient accuracy to solve the differential equation (4). Second, the coefficients of TdB/dT and T^2d^2B/dT^2 in Eq. (4) are smaller for polyatomic gases than for monatomic gases. For example, at 300 K, the coefficients for R134a are: $2(\gamma_0 - 1)^2/\gamma_0 = 0.0211$ and $(\gamma_0 - 1)^2/\gamma_0 = 0.011$. In contrast, the coefficients for argon are 0.667 and 0.267. For R134a the three terms in Eq. (4) contribute -1063, 27, and -59 cm^3/mol, respectively to β_a.

D. Alternative functional forms

In order to test the sensitivity of the determination of $B(T)$ from $\beta_a(T)$ to the functional form assumed for $B(T)$, alternative three-parameter functions were considered. A function of the form

$$B(T) = l\cdot[1 + (\epsilon/T)^p], \tag{15}$$

with the parameters: $l = -20.1$ cm^3/mol, $\epsilon = 911$ K, and

$p = 2.832$, represents the present $\beta_a(T)$ data and Weber's $B(T)$ with a standard deviation 1.6 times that given by Eq. (14). With the parameters mentioned, Eq. (15) differs from Eq. (14) by less than $0.005 \times B(T)$ throughout the temperature range $250 < T < 440$ K.

We attempted to fit the appropriate expressions resulting from the $(m,6,3)$ Stockmayer potential function to the $\beta_a(T)$ data and the $B(T)$ data. Very poor fits were obtained with $9 \leqslant m \leqslant 60$.

E. Third virial coefficient

The square-well potential leads to a closed-form representation for the third virial coefficient:[38]

$$C(T) = \tfrac{1}{8} b_0^2 (5 - c_1\Delta - c_2\Delta^2 - c_3\Delta^3), \tag{16a}$$

with

$$c_1 = r^6 - 18r^4 + 32r^3 - 15, \tag{16b}$$

$$c_2 = 2r^6 - 36r^4 + 32r^3 + 18r^2 - 16, \tag{16c}$$

$$c_3 = 6r^6 - 18r^4 + 18r^2 - 6, \tag{16d}$$

$$\Delta = \exp(\epsilon/kT) - 1, \tag{16e}$$

and $r \leqslant 2$. Equations (16), (4), (5), and (6), together with $\gamma_0(T)$ and the square-well parameters enumerated in the preceding section were used to calculate $\gamma_a(T)$. The resulting values of $\gamma_a(T)$ were roughly a factor of 2 more negative than the values of $\gamma_a(T)$ appearing in Table III. This demonstrates the limitations of the square-well potential when applied to R134a.

In an *ad hoc* effort to find an analytic representation for the present $\gamma_a(T)$ data and to test their consistency with Weber's $C(T)$ data, both sets of data were simultaneously fitted by Eqs. (4), (5), (6), and (16) to obtain a second model square-well potential, while retaining the first set of parameters for $\beta_a(T)$ and $B(T)$. For this fit, σ_{est} was chosen to be $0.045 \times \gamma_a(T)$ or $0.035 \times C(T)$, as appropriate. For the γ_a data, σ_{est} is approximately a factor of three times the standard deviations of γ_a listed in Table III. For the $C(T)$ data, σ_{est} is equal to Weber's estimate[39] of the systematic error from truncating virial expansion near 368 K. In fitting this second square-well model, Eq. (13) was used to calculate $\gamma_0(T)$. The regression led to the parameters: $b_0 = 206.6$ cm^3/mol, $\epsilon/k = 430.4$ K, and $r = 1.2661$. These parameters are so different from the parameters that fit the second virial data that no physical significance can be attributed to them. Figure 8 displays the data fitted, the deviations from the fit, and σ_{est}. Both sets of data show systematic deviations from this second fit and at 340 K there is an apparent inconsistency between the two sets of data which is approximately equivalent to 12% of C or 10% of $|\gamma_a|$ at 340 K. We are not able to identify the origin of this inconsistency. The inconsistency is barely changed when the representation of $C(T)$ is changed from Eq. (16) to polynomials in $1/T$; thus, the inconsistency does not appear to be a consequence of the particular functional form selected for $C(T)$.

In order to examine the sensitivity of $C(T)$ to systematic errors in the speed-of-sound data, it is useful to write a very rough approximation to Eqs. (4)–(6) which ignores all terms with factors of $\gamma_0 - 1$ or $\gamma_0^2 - 1$. One finds

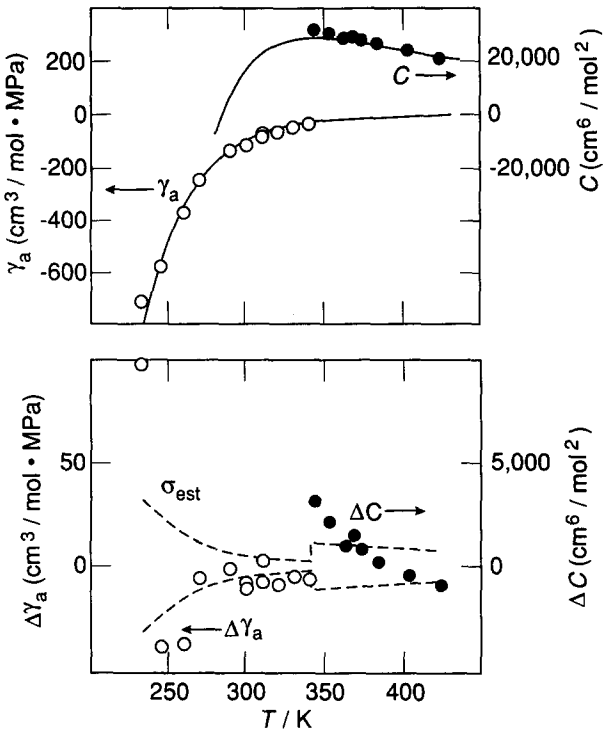

FIG. 8. Top: Measurements and "square-well" fits to the third virial coefficient C and the third acoustic virial coefficient γ_a as a function of temperature. The curves are calculated from Eq. (16) with the parameters: $b_0 = 206.6$ cm^3/mol; $\epsilon/k = 430.4$ K; $r = 1.2661$; and Eq. (14) with the parameters: $b_0 = 79.95$ cm^3/mol; $\epsilon/k = 601.6$ K; and $r = 1.2807$. Bottom: Differences between the measurements and the equations discussed in the text. The dashed curve labeled σ_{est} is the estimated standard deviation used to weight the data for fitting.

$$C(T) = \frac{\gamma_0}{1 + 2\gamma_0}(RT\gamma_a + \beta_a^2/2). \tag{17}$$

At 340 K, $RT\gamma_a \approx -112\,000$ cm^6/mol^2 and $\beta_a^2/2 \approx 150\,000$ cm^6/mol^2. These terms nearly compensate in Eq. (17) and this rough approximation implies that a fractional error of ϵ in γ_a produces an error of -3ϵ in C. Thus, the irreproducibility of γ_a observed upon changing samples is nearly large enough to account for the difference between $C(340\text{ K})$ deduced from the acoustic data and $C(340\text{ K})$ deduced by Weber from his Burnett data.

Despite the inconsistency, Eqs. (14) and (16) comprise our best estimates of B and C for R134a. Accordingly, Table IV. lists values of B and C calculated from these equations.

VI. THE VIRIAL EQUATION OF STATE DERIVED FROM $u(p,T)$

For the design of future measurement programs, it is of interest to consider the question: how accurately can the equation of state be determined from speed-of-sound data alone? To answer this question, we refitted Eqs. (14) and (16) to the values of β_a and γ_a appearing in Table II, without reference to Weber's data. Each datum was weighed inversely as the square of the standard deviation appearing in Table II. The square-well parameters that best fit $\beta_a(T)$ are: $b_0 = 65.215$ cm^3/mol, $\epsilon/k = 629.5$ K, and $r = 1.2964$, and the square-well parameters that best fit $\gamma_a(T)$ are: $b_0 = 184.26$ cm^3/mol, $\epsilon/k = 439.4$ K, and $r = 1.2671$. The

TABLE IV. Second and third virial coefficients of R134a from Eqs. (14) and (16) fitted to $u(T)$ and $p(V_m,T)$ data, simultaneously.

T/K	B/(cm^3/mol)	C/(dm^6/mol^2)
235	− 970.2	− 0.255
245	− 857.3	− 0.153
260	− 721.9	− 0.0641
275	− 616.4	− 0.0172
290	− 532.5	0.0074
300	− 485.7	0.0167
310	− 444.7	0.0225
320	− 408.7	0.0259
330	− 376.7	0.0277
340	− 348.3	0.0285
360	− 300.0	0.0280
380	− 260.6	0.0264
400	− 228.0	0.0244
420	− 200.6	0.0223
440	− 177.4	0.0205

deviations of the $u(p,T)$ data from the surface defined by these parameters are shown in Fig. 9. Clearly there is information in the acoustic data at higher pressures concerning higher virial coefficients which we have ignored.

The two sets of square-well parameters deduced from the acoustic data were used to calculate the virial coefficients B and C and they were used to calculate a truncated virial equation of state. In Fig. 10, this equation is compared to Weber's results, which include his values for the fourth ap-

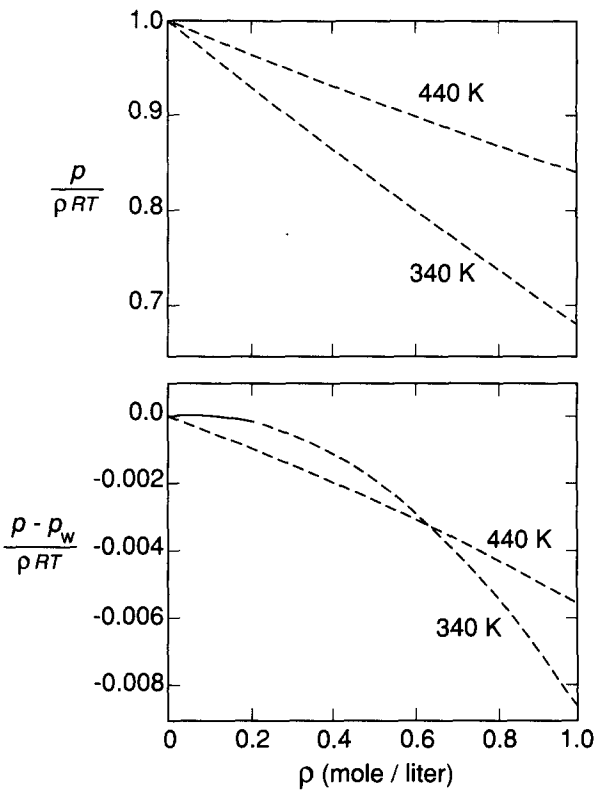

FIG. 10. Top: Two isotherms of R134a from Weber's data (Ref. 3). Bottom: The differences between the isotherms derived from the acoustic data and those determined by Weber. The solid curve indicates the range of the acoustic data. The dashed curves are extrapolations in density and/or temperature.

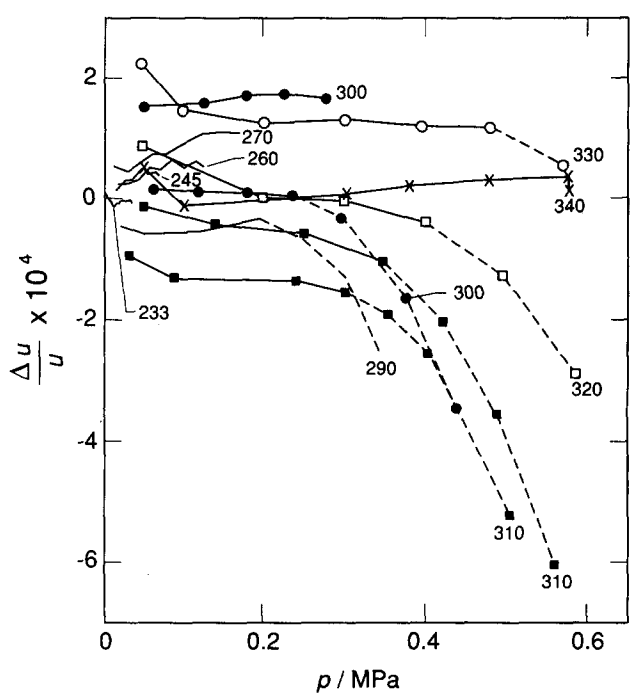

FIG. 9. Deviations $\Delta u = u(\text{measured}) - [(RT\gamma_0/M)\{1 + (\beta_a/RT)p + (\gamma_a/RT)p^2\}]^{1/2}$, scaled by $10^4/u$, with β_a and γ_a obtained from square-well functions fitted to the acoustic data alone. The curves drawn through the points are labeled by the temperature in Kelvin. The data connected by dashed lines were not used in fitting the three-term equation for each isotherm.

parent virial coefficient D. For the comparison, the compressibility factor $z = p/\rho RT$ is plotted as a function of ρ at 340 K, where the acoustic data nearly overlap Weber's $p(V_m,T)$ data, and also at 440 K, the highest temperature of Weber's data.

At 340 K the difference between the acoustic values of z and Weber's values is less than 0.000 18 in the range spanned by the acoustic data (0–0.22 mol/ℓ). The agreement is excellent. When the 340 K acoustic isotherm is extrapolated, a factor of 4.5 in density to the vapor pressure curve, the acoustic isotherm yields a value of z that is 0.0082 below Weber's value. This illustrates the good agreement of the acoustic value $B = -347.6$ cm^3/mol with Weber's value $B = -349.1$ cm^3/mol and poor agreement of the acoustic value $C = 22\,300$ cm^6/mol^2 with Weber's value $C = 32\,800$ cm^6/mol^2.

If the acoustic data are extrapolated 100 K upward in temperature to 440 K, the square-well parameters deduced from the acoustic data yield $B = -179.4$ cm^3/mol and $C = 17\,000$ cm^6/mol^2 which should be compared with Weber's results: $B = -175.3$ cm^3/mol and $C = 18\,800$ cm^6/mol^2. At 440 K and 2 MPa (0.6 mol/ℓ), the acoustic values of B and C lead to a value of z that is 0.0030 below the $p(V_m,T)$ value.

VII. SUMMARY

The speed of sound in gaseous R134a has been measured with an accuracy of approximately 0.01% in the temperature range $233 < T < 340$ K. From the data, $C^{pg}_{p,m}/R$ was deduced with an accuracy of approximately 0.1%. We have provided a three-parameter representation for the previously published second virial coefficient $B(T)$ and the present second acoustic virial coefficient $\beta_a(T)$ which falls within 0.5% of all the data within the temperature range $245 < T < 423$ K. We have determined the third acoustic virial coefficient $\gamma_a(T)$ with an imprecision of approximately 4.5% in the temperature range $245 < T < 340$ K; however, at 340 K the present value of γ_a appears to be inconsistent (by about 12% of γ_a) with previously published values of $C(T)$. The truncated virial equation of state derived solely from acoustic data is consistent with $p(V_m,T)$ data at 340 K within the density range spanned by the acoustic data. We have evidence the R134a is very soluble in certain elastomers.

ACKNOWLEDGMENTS

A.R.H.G. gratefully acknowledges the National Institute of Standards and Technology Guest Scientist appointment. This work was sponsored, in part, by the U.S. Department of Energy, Office of Buildings and Community Systems, the American Society of Heating, Refrigerating and Air-Conditioning Engineers, and the U.S. Environmental Protection Agency, Global Change Division. We are grateful to many colleagues for assistance. Dr. Donald Bivens of E. I. Du Pont de Nemours and Company supplied the R134a and Dr. T. Bruno of NIST analyzed it for air and water. Professor Ronald Aziz of the University of Waterloo provided tables of the properties of argon. Drs. Lloyd Weber and Graham Morrison of NIST provided unpublished details concerning their measurements of the properties of R134a. Dr. Keith Gillis recalibrated the resonator one year after this work was completed. Dr. Mike Ewing and Dr. Martin Trusler shared with us the computer programs they developed.

[1] M. O. McLinden, J. S. Gallagher, L. A. Weber, G. Morrison, D. Ward, A. R. H. Goodwin, M. R. Moldover, J. W. Schmidt, H. B. Chae, T. J. Bruno, J. F. Ely, and M. L. Huber, ASHRE Trans. **95**, Part 2, 263 (1989).
[2] Montreal Protocol on Substances that Deplete the Ozone Layer: Final Act, United Nations Environmental Programme (UNEP), Sept. 16, 1987.
[3] L. A. Weber, Int. J. Thermophys. **10**, 617 (1989).
[4] M. B. Ewing, A. R. H. Goodwin, M. L. McGlashan, and J. P. M. Trusler, J. Chem. Thermodynam. **19**, 721 (1987).
[5] M. B. Ewing, A. R. H. Goodwin, M. L. McGlashan, and J. P. M. Trusler, J. Chem. Thermodynam. **20**, 243 (1988).
[6] M. B. Ewing, A. R. H. Goodwin, and J. P. M. Trusler, J. Chem. Thermodynam. **21**, 867 (1989).
[7] A. R. H. Goodwin, Ph.D. thesis, University of London, Chemistry Department, 1988 (unpublished).
[8] J. B. Mehl and M. R. Moldover, in *Proceedings of the Eighth Symposium on Thermophysical Properties*, edited by J. V. Sengers (American Society of Mechanical Engineers, New York, 1982), pp. 134–141.
[9] M. B. Ewing and J. P. M. Trusler, J. Chem. Phys. **90**, 1106 (1989).
[10] M. R. Moldover, M. Waxman, and M. Greenspan, High Temp. High Press. **11**, 75 (1979).
[11] J. B. Mehl and M. R. Moldover, J. Chem. Phys. **74**, 4062 (1981).
[12] J. P. M. Trusler, Ph.D. Thesis, University of London, 1984 (unpublished).
[13] M. R. Moldover, J. B. Mehl, and M. Greenspan, J. Acoust. Soc. Am. **79**, 253 (1986).
[14] M. R. Moldover, J. P. M. Trusler, T. J. Edwards, J. B. Mehl, and R. S. Davis, J. Res. Natl. Bur. Stand. **93**, 85 (1988).
[15] M. R. Moldover and J. P. M. Trusler, Metrologia **25**, 165 (1988).
[16] M. B. Ewing, A. A. Owusu, and J. P. M. Trusler, Physica A **156**, 899 (1989).
[17] I. D. Campbell, Acustica **5**, 145 (1955).
[18] J. B. Mehl, J. Acoust. Soc. Am. **71**, 1109 (1982).
[19] J. P. M. Trusler (unpublished notes).
[20] *A.S.M.E. Boiler and Pressure Vessel Code Section VIII. Division 1 Pressure Vessels. ANSI/ASME BPV-VIII-1* (American Society of Mechanical Engineers, New York, 1986).
[21] In order to describe materials and experimental procedures adequately, it is occasionally necessary to identify commercial products by manufactures' name or label. In no instance does such identification imply endorsement by the National Institute of Standards and Technology, nor does it imply that the particular product or equipment is necessarily the best available for the purpose.
[22] T. J. Bruno, Thermophysics Division, NIST (private communication).
[23] J. B. Mehl and M. R. Moldover, J. Phys. Chem. **77**, 455 (1982).
[24] J. B. Mehl and M. R. Moldover, in *Topics in Current Physics*, edited by P. Hess (Springer, Berlin, 1989), Vol. 46, p. 61.
[25] M. B. Ewing, M. L. McGlashan, and J. P. M. Trusler, Metrologia **22**, 93 (1986).
[26] I. R. Shankland, R. S. Basu, and D. P. Wilson, in *Status of CFCs-Refrigeration Systems and Refrigerant Properties*, edited by D. R. Tree (International Institute of Refrigeration, Paris, 1988), pp. 305–314.
[27] R. G. Richard and I. R. Shankland, Int. J. Thermophys. **10**, 673 (1989).
[28] E. J. Owens and G. Thodos, Am. Inst. Chem. Eng. **6**, 676 (1960).
[29] D. D. Fuller, in *American Institute of Physics Handbook*, edited by D. E. Gray (McGraw-Hill, New York, 1972), pp. 2–64.
[30] R. C. Reid, and T. K. Sherwood, *The Properties of Gases and Liquids*, 2nd ed. (McGraw-Hill, New York, 1966), pp. 459–461.
[31] R. A. Aziz and M. J. Slaman, Mol. Phys. **58**, 679 (1986).
[32] R. J. Corruccini and J. J. Gniewek, *Thermal Expansion of Technical Solids at Low Temperatures*, U.S. Natl. Bur. Stand. Monogr. 29 (U.S. GPO, Washington, D. C., 1961).
[33] S. S. Chen, A. S. Rodgers, J. Chao, R. C. Wilhot, and B. J. Zwolinski, J. Phys. Chem. Ref. Data **4**, 441 (1975).
[34] R. S. Basu and D. P. Wilson, Int. J. Thermophys. **10**, 591 (1989).
[35] L. W. Bruch, Phys. Rev. **178**, 303 (1969); L. W. Bruch, Phys. Rev. A **2**, 2164 (1970).
[36] M. B. Ewing, M. L. McGlashan, and J. P. M. Trusler, Mol. Phys. **60**, 681 (1987).
[37] M. E. Boyd and R. D. Mountain, Phys. Rev. A **2**, 2164 (1970).
[38] T. Kihara, Nippon-Sugaku-Buturigakukaisi **17**, 11 (1943); J. O. Hirschfelder, C. F. Curtiss, and R. B. Bird, in *Molecular Theory of Gases and Liquids* (Wiley, New York, 1954), pp. 158–159.
[39] L. A. Weber (private communication).